

VALIDATION OF TWO NEW EMPIRICAL IONOSPHERIC MODELS IRI-PLAS AND NGM DESCRIBING CONDITIONS OF RADIO WAVE PROPAGATION IN SPACE

Maltseva Olga, Mozhaeva Natalia, Vinnik Elena

*Institute of Physics Southern Federal University, Stachki, 194, Rostov-on-Don, Russia
mal@ip.rsu.ru, mozh_75@mail.ru*

Keywords: GPS. Total electron content. Ionospheric model. Radio wave propagation. Geomagnetic disturbances. CHAMP. DMSP

Abstract: An empirical modeling of the behavior of ionospheric parameters is an important goal. The most complicated it is for the total electron content (TEC). The article focuses on two approaches: 1) the integration of N(h)-profiles using empirical parameters foF2 and hmF2, 2) the use of experimental values of the TEC. In recent years, two new models were developed: 1) IRI-Plas as a representative of the first approach, and 2) the Neustrelitz Global Model (NGM) as a representative of the second approach. Both models have their advantages over previous models. Any new model needs to be tested to get a quantitative estimate of proximity between the model and experiment, but both models have not been tested yet by anyone other than the authors of models. This article is dedicated to such testing. Besides the traditional comparison of model parameters foF2 and TEC with experimental data, in the paper the testing of additional parameters was performed with the help of independent experiments. For the IRI-Plas model, these are N(h)-profiles, data of incoherent scatter radars, and plasma frequency, measured at a height of satellites. For the NGM model, this is the equivalent slab thickness of the ionosphere τ . For the European region, it is shown that in most cases, the IRI-Plas model may be preferred to determine the parameters foF2 and TEC. For the parameter τ (NGM), there are conditions under which τ (NGM) provides better results than τ (IRI).

1 INTRODUCTION

Ionospheric models play an important role in determining wave propagation conditions of different frequency ranges in the nearest Earth space. The main parameters are the critical frequency foF2, the maximum height hmF2, the total electron content TEC. The most important parameter to operate navigation and communication systems is the TEC (e.g. Goodman, 2005). Positioning accuracy is directly proportional to the TEC. It can also be used to determine foF2 (Maltseva et al., 2012a). The article focuses on two approaches: 1) the integration of N(h)-profiles using empirical parameters foF2 and hmF2, 2) the use of experimental values of the TEC. The disadvantage of the first approach is the large discrepancy between model and experimental values of the TEC (Maltseva, Zhbakov, Nikitenko, 2011). In the second approach, there was no global empirical

model of the TEC, and the existing regional models provide a large range of values TEC (up to an order of magnitude) (e.g. Arican, Erol, Arican, 2003). In recent years, two new models were developed: 1) the IRI-Plas model (Gulyaeva, 2011) and 2) the Neustrelitz Global Model (Jakowski, Hoque, Mayer, 2011). In this paper, it is abbreviated by NGM. The IRI-Plas model refers to the first approach, the NGM model - to the second one. Both models have their advantages. The IRI-Plas model introduces the topside basis scale height Hsc, which improves the shape of the N(h)-profile, and takes into account a plasmaspheric part of the profile. As for the NGM model, according to (Jakowski et al., 2011) this empirical model can be operated autonomously without any ionospheric measurements. To characterize the solar activity dependency, the 10.7-cm flux of the Sun is used as a proxy for the ionizing extreme ultraviolet radiation. The model is easy to handle and can efficiently be used in single frequency GNSS and radar systems for estimating

range error or ionosphere related polarization changes by the Faraday effect. (p. 966).

Both models need to be tested, since no one other, than the authors themselves, did test these models. In this paper, testing will be conducted as to the common parameters (foF2 and TEC), allowing us to compare the results of both models to each other, and to the parameters that the authors did not test, but which are of great practical importance. In the first case, these are N(h)-profiles. They are tested by data of incoherent scatter radars and plasma frequency, measured at a height of satellites. In the second case, the model allows to determine the equivalent slab thickness of the ionosphere $\tau(\text{NGM}) = \text{TEC}(\text{NGM}) / \text{NmF2}(\text{NGM})$. This parameter also needs an empirical model but doesn't have it. The relevant test is to show whether can $\tau(\text{NGM})$ be an empirical model of the equivalent slab thickness of the ionosphere.

2 DATA AND MODELS USED

Experimental data of TEC values are used from the global maps of JPL, CODE, UPC, ESA, which are calculated from IONEX files (<ftp://cddis.gsfc.nasa.gov/pub/gps/products/ionex/>) for given coordinates and time points. Values of other parameters of the ionosphere were taken from the SPIDR database (<http://spidr.ngdc.nasa.gov/spidr/index.jsp>). Of the model, as indicated in the Introduction, there are two ones: IRI-Plas and NGM. The IRI model is well known and widely used. It is presented in some detail in the work (Maltseva, Mozhaeva, Zhbankov, 2012, below paper1) and in many others. Since the NGM model is completely new, it is necessary to give its brief description. A global model of the TEC(NGM) is given by product of five multipliers:

$$\text{TEC}(\text{NGM}) = F1 * F2 * F3 * F4 * F5.$$

It is based on data of the global CODE map. Each multiplier reflects the dependence of TEC on certain physical factors and is calculated using 2 to 6 coefficients CI. Coefficients are determined by the least-squares procedure superimposed on experimental data for several years. Coefficient F1 describes the dependence of TEC on the local time LT, i.e. on a solar zenith angle, and includes daily, half-day, 8-hour variations. It is calculated using 5 coefficients (C1-C5). Maximum of daily variations is shifted to LT = 14. Coefficient F2 describes annual and semi-annual variations, using coefficients C6-C7. Coefficient C8 is included in the

F3 multiplier describing the dependence of the TEC on the geomagnetic latitude. Coefficients C9 and C10 correspond to accounting equatorial anomalies in the latitude dependence of the TEC (factor F4). Coefficients C11 and C12 describe the dependence of the TEC on the index F10.7: $F5 = C11 + C12 * F10.7$. A model for NmF2 (Hoque and Jakowski, 2011) is built on the same principle, but has 13 coefficients, since in this case the factor F1 of daily course includes 6 coefficients. Maximum of daily variation is also shifted to LT = 14. A model of hmF2 (Hoque and Jakowski, 2012) includes 4 multipliers: $\text{hmF2} = F1 * F2 * F3 * F4$, because there is no special factor of the equatorial anomaly. F10.7 values are tied to the number of days of a year. Dependence on F10.7 is described by the factor F4. Below we give a comparison of parameters of the two models with experimental data and with each other. Results are represented using data of the Juliusruh station (in the main), located in the central part of Europe.

3 TESTING MODELS BY IS RADARS

As noted, because a value of TEC of the IRI model is calculated by integrating N(h)-profiles, it is important to test the profile shape with the help of independent experiments. One of them is incoherent scatter radars (ISR). Paper1 (Section 3) represented results of testing IRI-Plas according to three radars on the borders of the European zone near the maximum of solar activity. In recent years, much attention was paid to peculiarities of simulation results of ionospheric parameters and N(h)-profiles during periods of low activity (Cander and Haralambous, 2011; Liu et al., 2011; Zakharenkova et al., 2013; Cherniak et al., 2012; Maltseva, Mozhaeva, Nikitenko, Tinh Quang, 2012). This is all the more relevant as the forecast of maximum of the 24 cycle will be less than the maximum of the 23 cycle, and the 25 cycle will be even less powerful, as can be seen from Fig. 1 (from <http://solarscience.msfc.nasa.gov/predict.shtml>).

Data of the Kharkov radar (49.6°N, 39.6°E), located in the central part of Europe, allow to fulfill an additional test for the conditions of the minimum activity.

According to data for two years (2007-2008), the authors (Cherniak, Zakharenkova, Dzyubanov, 2013) were able to select only the two days: 25 September 2007 and 29 October 2008. Both days are

characterized by quiet geomagnetic conditions. Authors (Cherniak et al., 2013) compared critical frequencies foF2 of ISR with results of the Juliusruh station (54.6°N, 13.38°E).

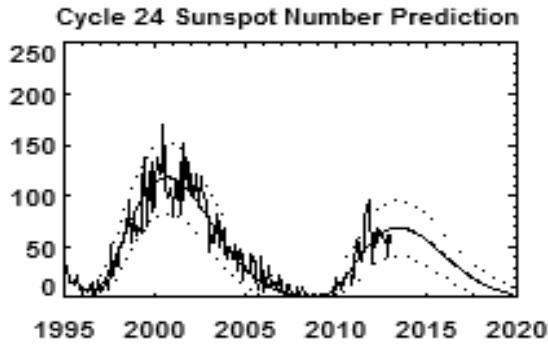


Figure 1. Solar number prediction for the 24 cycle

We compared them with results of the Pruhonice station (50°N, 14.5°E), which is closer to the Kharkov radar than the Juliusruh station. Fig. 2 shows the daily run of foF2 for the following cases: 1) monthly median of foF2 (icon “med”), 2) the experimental value (“obs”), 3) data of ISR, 4) values of foF2(rec), calculated using $\tau(\text{med})$ of the JPL map (Paper1), 5) the value of the original IRI model, which is the median, 6) the value of the NGM model. Unlike the IRI model, which uses moving 12-month indices RZ12, the NGM model formally defines not only the median (they just still need to be calculated from the values for the daily F10.7), but also the value for a particular day. The left panel refers to 29/10/2008, right – to 25/09/2007. In Fig. 3, these dependences are shown for the Juliusruh station.

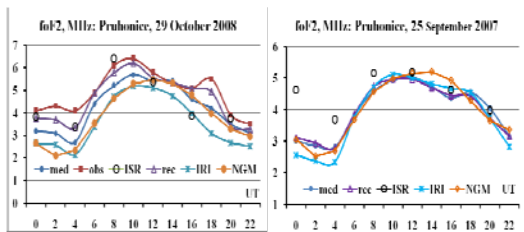


Figure 2. Comparison of various options of the foF2 determination (selected days, the Pruhonice station)

In Fig. 3, these dependences are shown for the Juliusruh station.

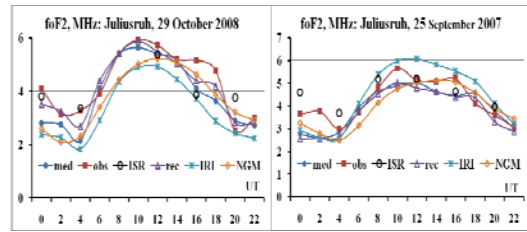


Figure 3. Comparison of various options of the foF2 determination (selected days, the Juliusruh station)

For completeness, the results are given for the Rostov station closest to the radar (data of this station were not available for October 2007), and Chilton at 09/25/2007 (fig. 4).

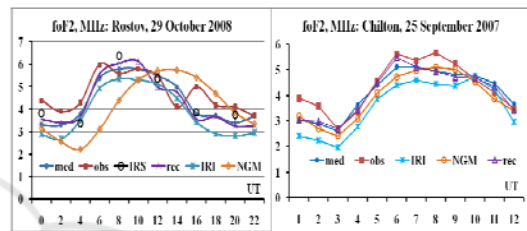


Figure 4. Comparison of various options of the foF2 determination (two stations)

Even these few graphs allow us to make some conclusions: with two exceptions of September 25, 2007 (2UT and 4UT), values for both models are fairly well with the experiment as medians and foF2 values on specific days. Quantitative deviations $|\Delta\text{foF2}|$ are minimal for foF2(rec) and maximum for foF2(IRI) or foF2(NGM). It is difficult to give preference to one of the models. For all 12 cases of ISR data, N(h)-profiles were calculated for the original model, and for adaptation of the model to the experimental values of various parameters, separately for cases of foF2, TEC and their joint use. Unlike paper1, an additional adjustment to the TEC(NGM) was added. The whole set of values of the TEC is shown in Fig. 5.

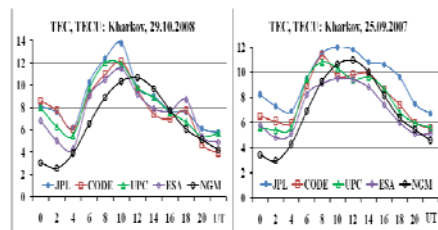


Figure 5. Comparison of various options of the TEC determination for the two days of Kharkov ISR measurements

Examples comparing N(h)-profiles with ISR profiles for the various options are shown in Fig. 6 for night (0 UT) and day (16 UT) conditions. This comparison has several objectives: a) to determine the map the N(h)-profile of which is the closest to the ISR profile, b) to determine the N(h)-profile for TEC(NGM).

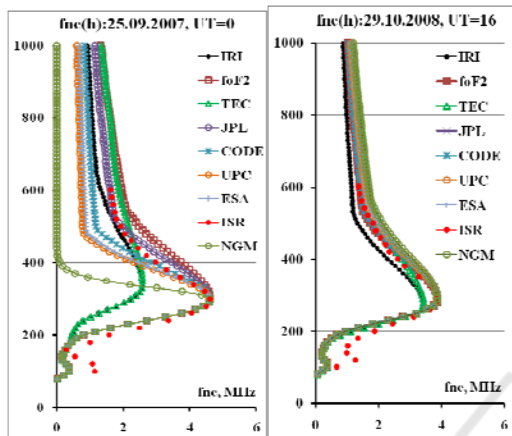


Figure 6. Comparison of N(h)-profiles calculated with N(h)-profiles of the Kharkov ISR

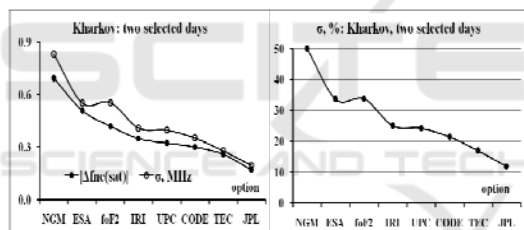


Figure 7. Comparison of model results with ones of global maps

It can be seen that the correspondence of N(h)-profiles are very different in day and night conditions. Daily profiles for all TEC options including TEC(NGM) are very close to the ISR profile. At night, only the N(h)-profile of the JPL map is close to the ISR profile. It is necessary to note that the JPL map gives the highest values of TEC. Profile for the NGM model shows virtually no ionization in the upper ionosphere, it is hard to imagine even in period of the minimum activity. A more complete picture is given by the analysis of all 12 cases. Fig. 7 (the left panel) shows the absolute deviations of the plasma frequency $fnc(600)$ and their dispersion (in MHz). They were obtained as the average for all days. The right panel displays the dispersion in %. This dispersion is important when comparing the results for different conditions of solar activity, because the relative dispersion is less

dependent on RZ12, than absolute. The values are sorted from maximum to minimum to highlight an option with the maximum and minimum deviation. We see that in this case, the maximum deviations correspond to the NGM model, minimum – to the JPL map. Fig. 8 shows the values of $fnc(h = 600)$ for the profiles of ISR, NGM and JPL (the left panel). The right side shows their deviation. The abscissa is date of the measurement for the two selected days.

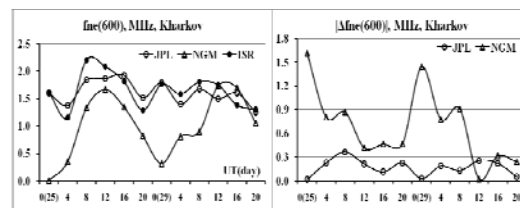


Figure 8. Comparison of plasma frequencies and their deviations for the two selected days and the two models

4 COMPARING THE CONFORMITY OF IONOSPHERIC PARAMETERS

Fig. 6 of the previous Section shows that the deviation of the JPL map does not exceed a certain value, and the NGM model is characterized by large deviations – at night. This Section provides an illustration of conformity of ionospheric parameters of the two models to the experimental data for the conditions of varying solar activity..

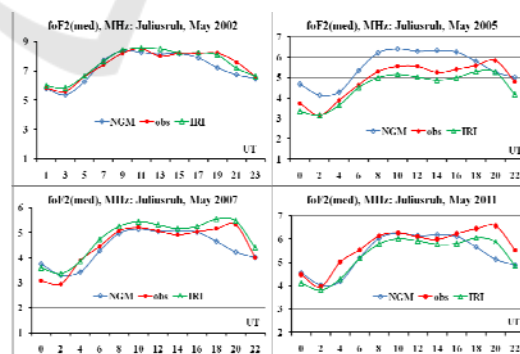


Figure 9. Examples of appropriate foF2 for different levels of solar activity (May, various years)

Comparison was made for medians of the corresponding parameters. Fig. 9 shows a comparison of foF2(med) for May. Fig. 10 represents results for December

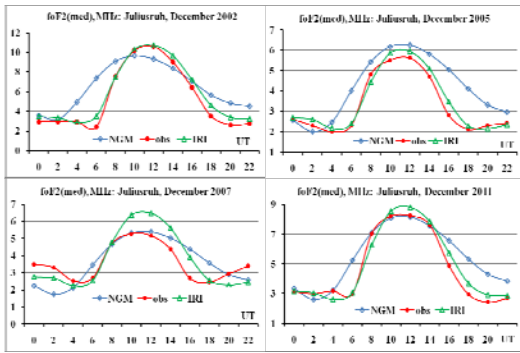


Figure 10. Examples of appropriate foF2 for different levels of solar activity (December, various years)

It is seen that in May and December the NGM model does not reflect the characteristics of diurnal values of foF2 (med). Examples of seasonal differences are shown in Fig. 11.

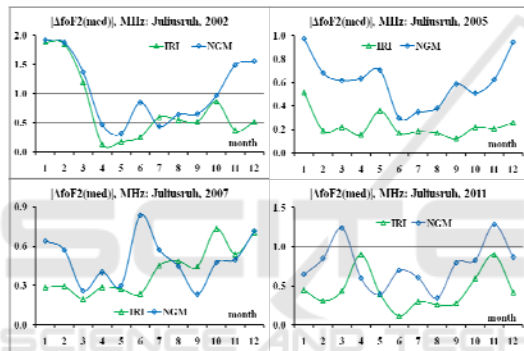


Figure 11. Examples of seasonal conformity foF2 for different levels of solar activity

Figures 12-14 represent similar results for the TEC. Here are experimental values of TEC(CODE). Additionally results of the JPL map are given, because its values are most commonly used in applications. For the IRI model, results are reported for 2 versions: IRI-Plas and IRI2001 (Bilitza, 2001).

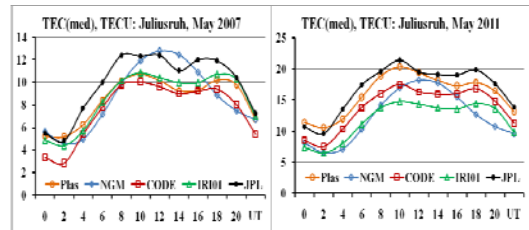
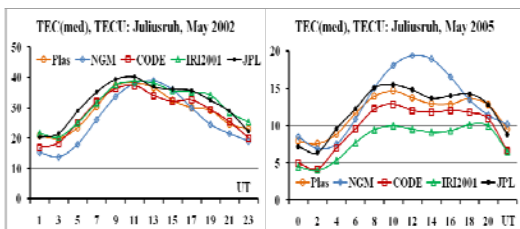


Figure 12. Examples of relevant TEC for different levels of solar activity (May, various years)

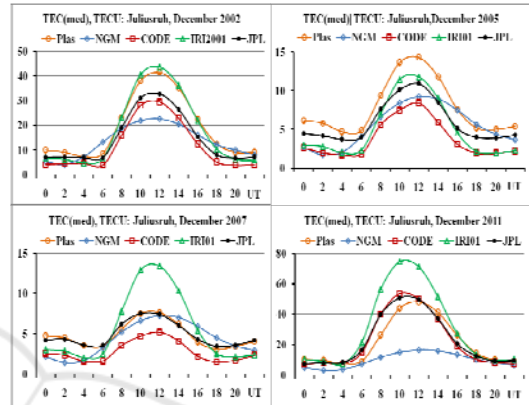


Figure 13. Examples of relevant TEC for different levels of solar activity (December, various years)

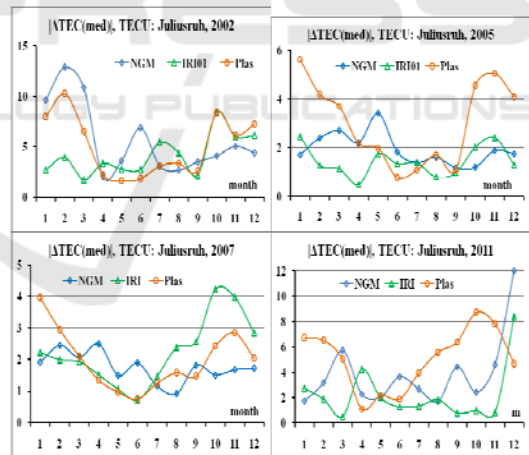


Figure 14. Examples of seasonal conformity of TEC for different levels of solar activity

As can be seen from Fig. 14, the value of this particular version is closest to the experimental TEC.

As for the two models, the IRI-Plas model often overestimates the value of TEC (compared with CODE), and hence gives greater deviations than NGM. Relative deviations in % are given in Table 1.

Table 1. Comparison of relative deviations for the two parameters of the ionosphere for the Juliusruh station

	y(foF2),%		y(TEC),%		
	NGM	IRI	NGM	IRI	Plas
2002	18.3	11.8	30.8	25.5	29.1
2005	17.7	6.5	34.3	29.7	56.0
2007	15.3	12.0	44.8	69.2	51.2
2008	19.0	20.0	96.3	57.0	125.
2011	18.1	10.3	40.7	27.8	62.7

As for the parameter hmF2, then it is more difficult to make the test for it, because experimental data are very limited. Fig. 15 shows the curves for maximum activity (May 2002, the Athens station) and for minimum (October 2008, the Juliusruh station).

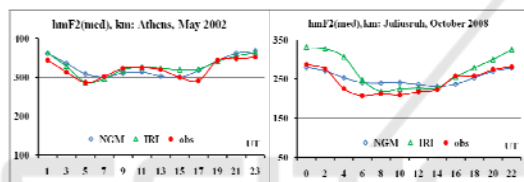


Figure 15. Examples of compliance of hmF2

On the one hand, there is a tendency inherent in the first two parameters: the deviation is less for both models in near maximum solar conditions, on the other hand, in both cases, the NGM model provides results that are 2 times better than the IRI (relative deviations are 5 and 10% in the first case and 8 and 15% in the second one.)

5 COMPARISON OF RESULTS FOR THE MEDIAN OF THE EQUIVALENT SLAB THICKNESS OF THE IONOSPHERE $\tau(MED)$

Parameter τ ($= TEC/NmF2$) may play a role in assessing the state of the ionosphere. In (Gulyaeva, 2011), a formula between parameters Hsc (the topside basis scale height) and foF2 was obtained, allowing (maybe) to predict the behavior of this parameter during disturbances. Since there is a relationship between τ and Hsc (Hsc is a part of τ), it is possible, apparently, to get a connection for τ . But

in this work, as in the paper1, we focus on assessing the possibility of determination of foF2 from experimental TEC with $\tau(med)$. Traditional methods are based on the use of $\tau(IRI)$ (McNamara, 1985; Houminer and Soicher, 1996; Gulyaeva, 2003), i.e. $NmF2(rec) = TEC(obs)/\tau(IRI)$. Frequency foF2(rec) is proportional to the square root of NmF2(rec). Naturally, the calculated values NmF2(rec) will be the closer to the experimental NmF2(obs), the closer $\tau(IRI)$ to $\tau(obs)$.

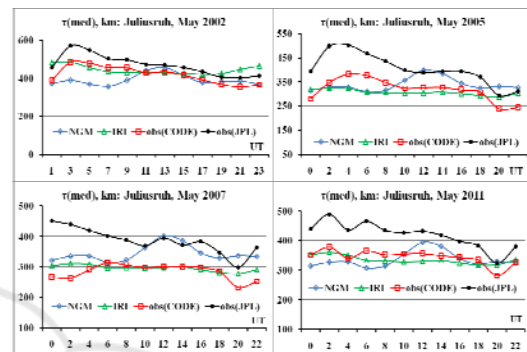


Figure 16. Examples of appropriate $\tau(med)$ for different levels of solar activity (May, various years)

In this section, these values are determined for the NGM model, to compare the experimental values (defined from the CODE map) with $\tau(IRI)$ and $\tau(NGM)$. Additionally they show $\tau(JPL)$, since in most cases this map gives the best fit to the experimental data of foF2. The corresponding results are shown in Fig. 16-17, which are obtained using curves of Figs 9-10, 12-13.

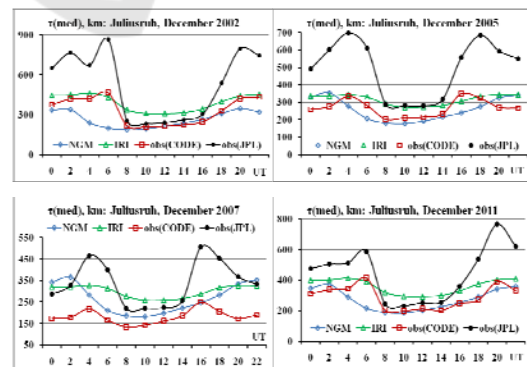


Figure 17. Examples of appropriate $\tau(med)$ for different levels of solar activity (December, various years)

These large differences between $\tau(CODE)$ and $\tau(JPL)$ should not be discouraged, because they are obtained from different TEC (TEC(CODE) and

TEC(JPL)). Authors (Jakowski et al., 2011) selected the CODE map. If they chose the JPL map, the results would have been closer to $\tau(\text{JPL})$. As can be seen from these Figures, almost all the values of $\tau(\text{NGM})$ are closer to the experimental $\tau(\text{CODE})$, than $\tau(\text{IRI})$, therefore, $\text{foF2}(\text{rec})$ for $\tau(\text{NGM})$ should be closer to the $\text{foF2}(\text{obs})$ than $\text{foF2}(\text{IRI})$. To confirm this important fact and assess the possible use of $\tau(\text{NGM})$ for the determination of foF2 , calculations were fulfilled for IRI, NGM, and different maps (Fig. 18).

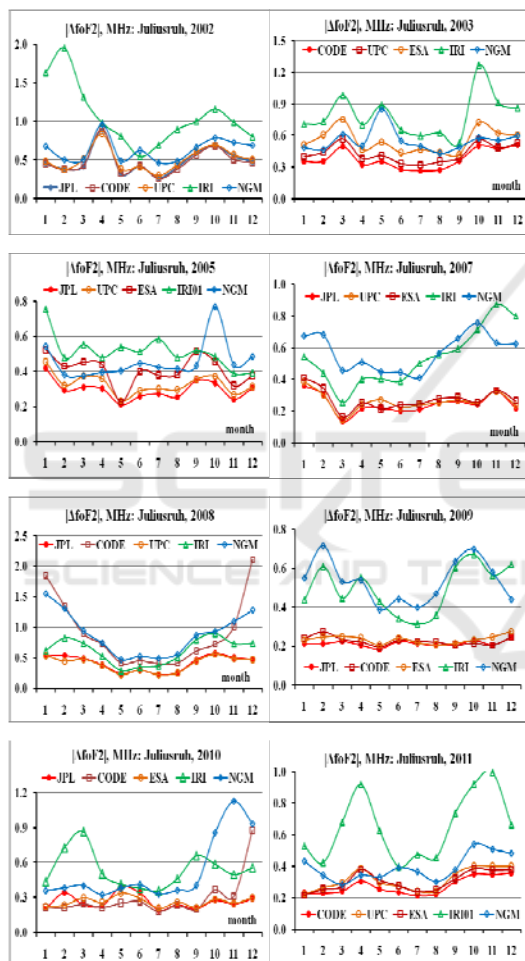


Figure 18. The absolute difference between experimental frequencies foF2 and frequencies calculated using the values of medians of τ for global maps of JPL, CODE, UPC, ESA and empirical models IRI and NGM

It turned out that the results depend on the level of solar activity, so we have provided detailed graphs for several years to illustrate what the conditions are most favorable for $\tau(\text{NGM})$. Each graph shows the absolute difference between

experimental values $\text{foF2}(\text{obs})$ and values $\text{foF2}(\text{rec})$, recovered using appropriate TEC. The general trend is to ensure that, in determining $\text{foF2}(\text{rec})$ from the TEC best results are obtained for the JPL map. The "second" place belongs to the CODE map. As for NGM, then its deviations $|\Delta\text{foF2}|$ are much smaller than these for the model IRI under the conditions of high solar activity though they are larger in magnitude than deviations for global maps. As already noted, the simulation results in low solar activity is of great interest because of the evidence found that the model IRI is worse working in these conditions (2007-2009) (Zakharenkova et al., 2011; Maltseva et al., 2012a). Fig. 18 shows that the NGM model does not improve results compared with the IRI model. In addition, results for 2008 (the year with the lowest activity) show that the determination of the TEC from the CODE map reveals a significant effect of measurement error on the values themselves (apparently, the value of error is much greater than the TEC for this map)

6 TESTING MODELS USING PLASMA FREQUENCIES MEASURED BY SATELLITES

Paper1 has attempted to test the IRI model by data of CHAMP ($h \sim 400$ km) and DMSP ($h \sim 860$ km) satellites. It has been shown that in most cases $N(h)$ -profiles corresponding to various maps do not provide an exact match of the plasma frequency $f_{\text{ne}}(\text{sat})$ at the height of the satellite, but one can choose a profile that passes through the $\text{foF2}(\text{obs})$ and plasma frequency of one or two satellites. This yields a value of TEC, other than the maps. In most cases, these values fall in the range of maps and form there an own subset. We use the $f_{\text{ne}}(\text{sat})$ to evaluate the situation for the NGM model. The results are shown in Fig. 19 for stations Juliusruh and Chilton and the various levels of solar activity. The red circles show the values of $\text{TEC}(f_{\text{ne}})$ for $N(h)$ -profiles passing through $f_{\text{ne}}(\text{sat})$ of the DMSP satellite. The remaining values correspond to global maps (no values of the UPC map, because they are very close to the values of CODE). Values of TEC are ordered from maximum to minimum for each hour of UT, shown on the horizontal axis.

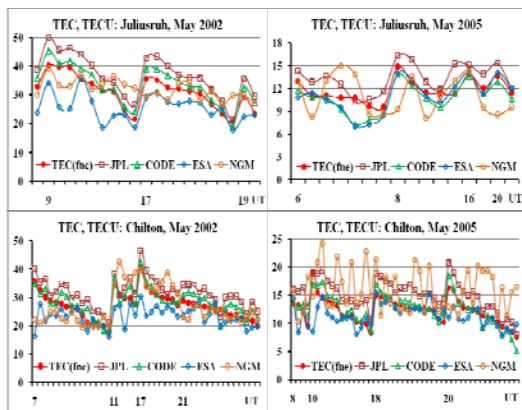


Figure 19. A comparison of different sets of TEC

Fig19 shows: a) the range of possible values for each of the experimental hour is large, b) TEC is experiencing great changes for various days and one hour, but changes are sufficiently synchronized for all maps. NGM model values, in-first, go far beyond the experimental range, to-second, within the hour have large random variation in various days.

7 EXAMPLES OF THE DISTURBED BEHAVIOR OF N(h)-PROFILES

Examples of the disturbed behavior of N(h)-profiles are represented in Fig. 20 during the last disturbance of May 2005. The strongest phase of this disturbance falls on 30 May. One can see response of various parts of N(h)-profiles on this disturbance in different latitudes. The top panel concerns to the Juliusruh station. The middle panel displays results for the Sofia station. The part of them was given from paper1 (fig. 10) to compare with new results. The bottom panel concerns to the Athens station. All profiles are close to model ones in 4UT (near quiet conditions). In the next moments 10-14UT, the positive disturbance over the Juliusruh station is developed covering only topside profiles. N(h)-profiles over the Sofia station show redistribution of ionization, i.e. its increase near hmF2 due to depletion of the higher part. Conditions over the Athens station are characterized by input of ionization from the magnetosphere (10UT), two-fold increased ionization of the whole profile (12UT). Phase of recovering (31 May) is faster in the topside part than in the bottom of the F2 layer, where the negative disturbance continues during all day. It shows that N(h)-profiles of the IRI-Plas model can

be used not only in technical applications but to solve some problems of physics of the ionosphere.

8 CONCLUSION

The paper discusses two new models that give average values of ionospheric parameters: the critical frequency foF2, the maximum height hmF2, the total electron content TEC. One of them is the IRI-Plas model, which is a new option of the IRI model, the best known and most widely used, which is constantly updated. Its additional testing was held according to the Kharkov IS radar and the satellite data in a period of low solar activity. The second one is the new NGM model (the Neustrelitz Global Model), which is extremely simple: each parameter is the product of no more than 5 factors: $P = F1 * F2 * F3 * F4 * F5$ with clear physical binding of each factor. Another feature of the model is the dependence of each parameter on the number of days in the year and the corresponding index F10.7. To build the model TEC, its authors selected the global CODE map. Results obtained confirm the findings of the paper1 concerning to the high efficiency of adaptation of the IRI-Plas model to the experimental values of foF2, hmF2, and TEC. Further adaptation to the plasma frequency fne, measured by satellite DMSP, leads to new values of TEC(fne), which fall in the range of experimental values of global maps and can be considered as an independent estimate of the TEC. As regards the NGM model, for the purposes of its authors, i.e. in single frequency GNSS and radar systems, it is possible that the simplicity of the model plays a crucial role and the model will be used with success. In principle, the average foF2 and TEC values are predicted well, and in some cases the NGM model can give better results than IRI. But for the purposes of the wave propagation this is not enough, because the NGM model does not reflect daily variations of foF2 and TEC, and the discrepancy with the experimental data and with the IRI model may be 1.5-3 times.

It should be noted that in some cases the best results for the TEC are provided by the IRI2001 model, whose ceiling of N(h)-profile is 2000 km. This is due to the fact that the IRI2001 model strongly overestimates the concentration in the upper ionosphere (up to 1000 times) and this compensates for the lack of the plasmaspheric part of the N(h)-profile. Apparently, the fact that the new IRI-Plas

option also overestimates TEC in some cases, suggests that the real Hsc of the new profile is smaller than the model Hsc. As for the median equivalent thickness of the ionosphere $\tau(\text{med})$, then there are conditions of solar activity, when the NGM model gives results better than the IRI model. Such a conclusion cannot be generalized to other regions without additional testing because of a strong dependence of the results on the location of the

observation point and the solar activity. We can note also that previous versions of the IRI model (IRI2001 (Bilitza, 2001) and IRI2007 (Bilitza and Reinisch, 2008)) were validating during tens of years and this validation is continued. Validation of the IRI-Plas model and the NGM model began just now.

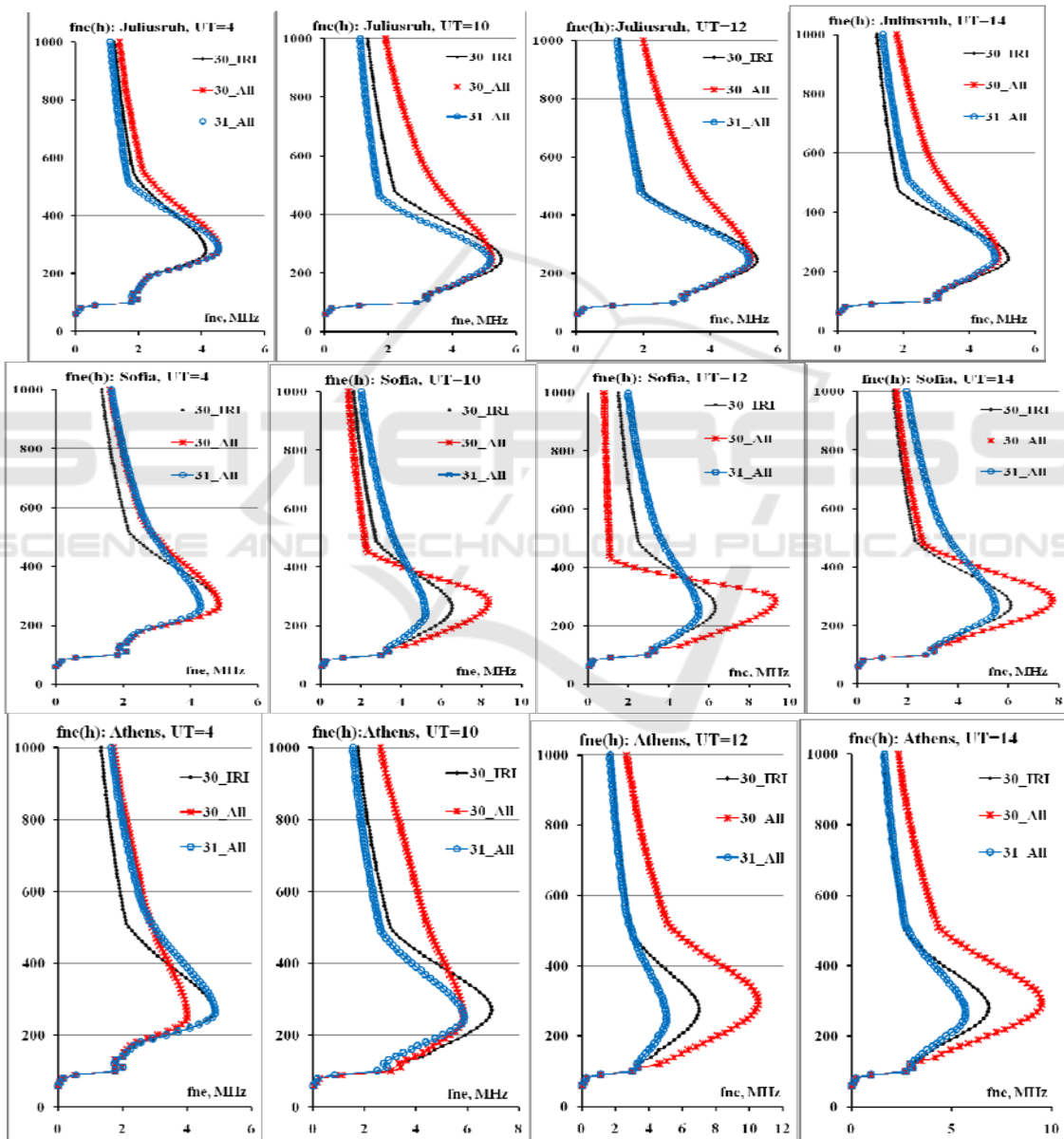


Figure 20. Development of disturbance of 30-31 May 2005 in N(h)-profiles on different latitudes

ACKNOWLEDGEMENTS

Authors thank organizations and scientists who are developing the IRI model, providing data of SPIDR, JPL, CODE, UPC, ESA, Dr M. Hoque for detailed comments on the NGM model, two reviewers for useful comments.

REFERENCES

- Arikan, F., Erol, C. B., Arikan, O. (2003). *Regularized estimation of vertical total electron content from Global Positioning System data*. Journal of Geophysical Research, 108(A12), 1469, doi:10.1029/2002JA009605.
- Bilitza, D. (2001). *International Reference Ionosphere*. Radio Science, 36(2), 261-275.
- Bilitza D., Reinisch, B.W. (2008). *International Reference Ionosphere 2007: Improvements and New Parameters*. Advances in Space Research, 42, 599-609.
- Cander, L.R., Haralambous, H. (2011). *On the importance of TEC enhancements during the extreme solar minimum*. Advances in Space Research, 47, 304-311.
- Cherniak, Iu.V., Zakharenkova, I.E., Dzyubanov, D.A. (2013a). *Accuracy of IRI profiles of ionospheric density and temperature derived from comparisons to Kharkov incoherent scatter radar measurements*. Advances in Space Research, 51(4), 639-646.
- Cherniak, Iu.V., Zakharenkova, I.E., Krankowski, A., Shagimuratov, I.I. (2012b). *Plasmaspheric electron content from GPS TEC and FORMOSAT-3/COSMIC measurements: solar minimum conditions*. Advances in Space Research, 50(4), 427-440.
- Goodman, J.M. (2005). *Operational communication systems and relationships to the ionosphere and space weather*. Advances in Space Research, 36, 2241-2252.
- Gulyaeva, T.L. (2003). *International standard model of the Earth's ionosphere and plasmasphere*. Astronomical and Astrophysical Transaction, 22(4), 639-643.
- Gulyaeva, T.L. (2011). *Storm time behavior of topside scale height inferred from the ionosphere-plasmasphere model driven by the F2 layer peak and GPS-TEC observations*. Advances in Space Research, 47, 913-920.
- Hoque, M.M., Jakowski, N. (2011). *A new global empirical NmF2 model for operational use in radio systems*. Radio Science, 46, RS6015, 1-13.
- Hoque, M.M., Jakowski, N. (2012). *A new global model for the ionospheric F2 peak height for radio wave propagation*. Annales Geophysicae, 30, 797-809.
- Houminer, Z., Soicher, H. (1996). *Improved short-term predictions of foF2 using GPS time delay measurements*. Radio Science, 31(5), 1099-1108.
- Jakowski, N., Hoque, M.M., Mayer, C. (2011). *A new global TEC model for estimating transionospheric radio wave propagation errors*. Journal of Geodesy, 85(12), 965-974.
- Liu, L., Chen, Y., Le, H., Kurkin, V.I., Polekh, N.M., Lee, C.-C. (2011). *The ionosphere under extremely prolonged low solar activity*. Journal of Geophysical Research, 116, A04320, doi:10.1029/2010JA016296.
- Maltseva, O., Mozhaeva, N.S., Nikitenko, T.V., Think Quang T. (2012a). *HF radio wave propagation in conditions of prolonged low solar activity*, Proceedings of IRST2012, York, P07, 1-5.
- Maltseva, O.A., Mozhaeva, N.S., Poltavsky, O.S., Zhbakov, G.A. (2012b). *Use of TEC global maps and the IRI model to study ionospheric response to geomagnetic disturbances*. Advances in Space Research, 49, 1076-1087.
- Maltseva, O., Mozhaeva, N., Zhbakov, G. (2012c). *A new model of the International Reference Ionosphere IRI for Telecommunication and Navigation Systems*. Proceedings of the First International Conference on Telecommunication and Remote Sensing, 129-138.
- Maltseva, O.A., Zhbakov, G.A., Nikitenko, T.V. (2011). *Effectiveness of Using Correcting Multipliers in Calculations of the Total Electron Content according to the IRI2007 Model*. Geomagnetism and Aeronomie, 51(4), 492-500.
- McNamara, L.F. (1985). *The use of total electron density measurements to validate empirical models of the ionosphere*. Advances in Space Research, 5(7), 81-90.
- Zakharenkova, I.E., Krankowski, A., Bilitza, D., Cherniak, Yu.V., Shagimuratov, I.I., Sieradzki, R. (2013). *Comparative study of foF2 measurements with IRI-2007 model predictions during extended solar minimum*. Advances in Space Research, 51(4), 620-629.